Acta Crystallographica Section A
Foundations of Crystallography
ISSN 0108-7673

Received 4 December 2001
Accepted 10 December 2001

Wavelength extrapolation to zero extinction: a γ-ray case. The quantitative effect of the extrapolation function on the kinematical limit value

A. McL. Mathieson[a,b]* and A. W. Stevenson[b]

[a]Chemistry Department, La Trobe University, Bundoora, Victoria 3083, Australia, and [b]CSIRO Manufacturing Science and Technology, Private Bag 33, Clayton South MDC, Victoria 3169, Australia. Correspondence e-mail: s.mathieson@latrobe.edu.au

To ensure that a true zero-extinction kinematical limit value has been attained by extrapolation of a series of measurements on one reflection, the proper dependence of a function of F *versus* the function of the physical variable involved in the measurements has to be identified. To demonstrate this point, the multiwavelength γ-ray data on seven reflections of NiF_2 reported by Palmer & Jauch [*Acta Cryst.* (1995), A**51**, 662–667] have been utilized. A new physical component has been introduced into the relationship between diffracted intensity and wavelength – that due to the decrease in angular divergence of diffraction from crystallites with decrease in wavelength. For γ-rays, this leads to a function of F^2 in respect of wavelength, *viz* $F^2 = F_0^2 - \alpha\lambda + \beta\lambda^2$, which is different from that derived from Zachariasen-type models, *viz* $F^2 = F_0^2 - k\lambda^2$. Comparison of the limit values according to Palmer & Jauch and according to Mathieson & Stevenson demonstrates the advantage of the functional dependence proposed in this study.

1. Introduction

With γ-rays of wavelength 0.0205, 0.0265, 0.0392 and 0.0603 Å, Palmer & Jauch (1995), hereafter PJ95, measured the diffracted intensities from a group of seven reflections from a single crystal of NiF_2 (recorded as F^2 in their Table 1). The sets of four results were tested by Palmer & Jauch against the predictions from extinction models of Becker & Coppens (1975) and of Sabine (1992) to determine which was more in accord with the experimental data. Our intention is different. With this unique set of γ-ray data, we have examined the question of extrapolation to zero extinction (Mathieson, 1979; Mackenzie & Mathieson, 1979, 1984) in respect of wavelength in the γ-ray region. To this end, we have considered the role of changing wavelength on the conditions of diffraction from the assembly of crystallites of an 'imperfect crystal'.

2. The role of extrapolation

Extrapolation of a series of experimental measurements, $A_n(a_m)$, against a function of the variable, a, to a specified limit, a_L, which is not itself attainable directly by experimental means, can be a valuable procedure to establish a 'correct' value of A, correct in the sense either of the elimination of systematic errors in A_n and/or the achievement of a proper prescription of A. The selection of the most appropriate function of the variable can influence the value at the extrapolation limit and is therefore a matter of some importance.

In crystallography, use has been made of this procedure to establish accurate estimates of cell parameters by extrapolation to $\theta = 90^\circ$ on the basis that the various sources of systematic error are eliminated at the otherwise-unattainable limit [see Buerger (1942) for the development of this approach]. Initially, the extrapolation procedure (Kettmann, 1929) was pragmatic and involved a series of measurements plotted against θ, with graphical extrapolation to $\theta = 90^\circ$.

Subsequently, extrapolation to that limit was against different functions of θ (or a combination of such functions), the particular function being related to the specific source of the systematic error. In other words, the form of the function used for reliable extrapolation depends on the specific characteristics of the experimental set-up, including those of the specimen.

When one's concern is with the attainment of accurate zero-extinction kinematical limit structure-factor values by extrapolation (Mathieson, 1979; Mackenzie & Mathieson, 1979, 1984), then, as noted above, the form of the function of the variable selected can be critical. In the present context, it is therefore of importance to look at the physical factors involved in diffraction in the very short wavelength γ-ray region.

When diffraction from imperfect crystals with γ-rays of wavelength less than 0.1 Å is compared with diffraction with

Table 1
Width of beam divergence, $\theta' - \theta''$, with respect to the γ-ray wavelength.

λ (Å)	Width ($\theta' - \theta''$) ($''$)
0.02	4.1
0.04	8.3
0.06	12.4
0.08	16.5
0.10	20.6
1.00	206.4

more conventional wavelengths *ca* 1 Å, the comparative magnitude of certain factors is altered. Thus the role of absorption is much reduced and the relative role of scattering rendered more significant. In particular, the reduction in wavelength relative to the size of the constituent crystallites influences the divergence of the beams diffracted by the crystallites.

If we look closely at the features subsuming the various models derived from Darwin's (1922) equations, such as those referred to in PJ95, there appear to be two main aspects that invite question. Firstly, the matter of wavelength is not explicitly included in the equations. So relationships derived solely from Darwin's equations, and subsequent variants, do not and cannot yield a functional relationship in respect of wavelength. Only when allied with other factors, *e.g.* as derived from Zachariasen's (1967) treatment, does a dependence of extinction level on wavelength appear to apply, as utilized in PJ95 (p. 665) $-\gamma\,(\lambda) = (1 - k\lambda^2)$. Secondly, there is an in-built contradiction between the physical model – the 'mosaic' crystal, made up of an array of fragmented crystallites – and the mathematical model based on differential calculus. The mathematical model presumes a continuous medium, *i.e.* a continuous dependence of scattering per unit length, while the physical model is such that the sequence of interactions may occur after a distance that may be short or long.

So we have concluded that, to examine the dependence on λ, we will accept the essential physical nature of the 'mosaic' model but consider an approach that is compatible with the probable steps when a γ-ray beam passes through an array of crystallites – namely a sequence of discontinuous interactions.

3. The discontinuous model

In order to establish the picture in relation to γ-ray diffraction by an 'imperfect' crystal, examination of the situation *ab initio* in some detail is necessary. First, consider an individual crystallite.

3.1. The acceptance and diffraction angular ranges of a crystallite

Imagine a vanishingly thin vertical line source of radiation of wavelength λ. Let there be a small crystallite on a vertical rotation axis. Associated with a particular Bragg plane of the crystallite is an acceptance arc, origin at the crystallite and looking towards the source with a divergence angle φ_a. There is also the diffraction arc, centred at the crystallite and pointing towards the detector, with a divergence angle φ_d. When the crystallite is rotated on its axis, the acceptance and diffraction arcs also rotate. When the acceptance arc intercepts the source, radiation is transmitted from the source to the crystallite and is then diffracted at the edge of the diffraction arc. This continues as the crystal rotates until the acceptance arc reaches its limit and passes beyond the source. Simultaneously, the diffracted beam reaches the outer edge of the diffraction range.

3.2. The magnitude of φ in relation to λ

Consider diffraction from a crystallite of dimension 1000 Å (say), where d is the plane spacing and N is the number of planes so Nd = 1000 Å. In respect of this one dimension, the width of the divergence of the first-order reflection of spacing d is given by the Wilson–Stokes relationship (Wilson, 1949):

$$\theta' - \theta'' = \lambda/\varepsilon \cos\theta, \qquad (1)$$

where ε represents the thickness of the crystallite. It is evident that the beam divergence from a crystallite, φ_d, as given by $\theta' - \theta''$, is proportional to the wavelength, see also James (1948). Table 1 shows the variation of the width for the change in λ from 0.02 to 0.10 Å.

It should be noted that, for conventional X-ray wavelengths such as 1 Å, the value of the width, see Table 1, may be comparable with the misorientation distribution of crystallites so that the following discussion would be modified in that region. The conditions associated with a merging into the region of X-ray wavelengths remain to be explored.

At this stage, we ignore the absorption factor.

3.3. Impact of the dimension of φ_d on diffraction from a crystal block of crystallites

Fig. 1(i) schematically depicts the sequence of interactions with crystallites in a mosaic crystal. For the first interactions (Fig. 1*a*), the angular scan range of the crystal block is greater than the limits of the orientational distribution of the crystallites ('mosaic spread') so, when the crystal block is rotated, the acceptance arcs of all crystallites have the opportunity to interact with the source. This is only true of the first interactions. The result may be depicted in Fig. 1(*a*)(ii) where the crystallites are shown distributed throughout the crystal, z representing the distance through the crystal from the entrance face to the exit face, z_L. Crystallite interaction is indicated by their 'lighting up' and, for this interaction, every crystallite interacts so the level of interaction through the crystal block is shown as constant [Fig. 1(*a*)(iii)]. The resultant diffracted intensity corresponds to the first term, I_1.

Subsequent interactions after the first are of a different nature. Instead of a broad source of X-rays, the radiation passed on after the first interactions consists of an array of beams from the individual crystallites distributed throughout the crystal block and with divergence determined by the crystallites' size and hence the wavelength, see equation (1). These beams are then incident on the fixed mutual orientational distribution of the crystallites within the crystal block.

So subsequent interactions depend on two factors – the divergence of the acceptance/diffracted beams and the distribution of crystallite orientations. Not all subsequent potential interactions (from a purely angular point of view) can take place because the probability of interaction occurring will change as one goes from the entrance face of the block to the exit face.

The second interactions (Fig. 1*b*) can only happen after the first interactions so the level of interaction at $z = 0$ is zero. Beams that arise from first interactions throughout the crystal will then proceed forward through the crystal block. The level of interaction increases with passage through the crystal. Since the beams diffracted by the first interaction are of much smaller divergence compared with the 'mosaic spread' of the crystallites, the number of crystallites that are activated or partially activated ('lit up' in the diagram) [Fig. 1(*b*)(ii)] is much reduced and, *in toto*, is proportional to the divergence and hence to λ. So the normalized diffracted intensity of this component is $I_2 = -\alpha\lambda$. The general trend of the level of interaction for the second interactions is indicated in Fig. 1(*b*)(iii).

The population of beams to generate the third interaction (Fig. 1*c*) is proportional to λ. These beams, in their turn, interact with the mosaic spread of crystallites that lie between them and the exit face. The overall effect is multiplicative and the number of interactions is therefore much reduced [Fig. 1(*c*)(ii)] so that the normalized diffracted intensity component is $I_3 = +\beta\lambda^2$. The corresponding trend of the level of interaction for the third interactions is indicated in Fig. 1(*c*)(iii). So the normalized intensity in the diffracted beam corresponds to $F^2 = F_0^2 - \alpha\lambda + \beta\lambda^2$.

This model suggests a form of extrapolation appropriate for multiwavelength γ-ray data. It also indicates that it could provide estimates of the second and subsequent interaction components (if any).

3.4. Examination of the PJ95 data

To examine the experimental data of PJ95 in relation to the 'discontinuous model', the first step was simply to plot the data against λ. This proved most interesting in that it revealed that, even within this limited sample of seven reflections, there were clear-cut differences. For five of the seven (Fig. 2*a*), they rather obviously suggest straight line relationships, $F^2 = F_0^2 - \alpha\lambda$, the lines fitted by least squares being shown. By their linear nature, it is evident that extrapolation to $\lambda = 0$ yields proper estimates of the zero-extinction F_0^2 values for the individual reflections. For these five reflections, the discontinuous model indicates that only the first and second interactions are relevant and any subsequent interactions do not apparently make a significant contribution.

With respect to the remaining two reflections, again the experimental data are plotted against wavelength (Fig. 2*b*). In this case, the experimental points do not fall on a straight line but are curved concave upwards. While approximately holding to a straight line near $\lambda = 0$, the curves bend upwards as λ increases indicating a positive contribution to F^2. In the discontinuous model, this corresponds to the positive contribution from the third interaction. Fitted values for these latter two reflections are shown in Table 2, which also presents the individual λ and λ^2 contributions. [Note: There is no presumption that the experimental points are absolutely

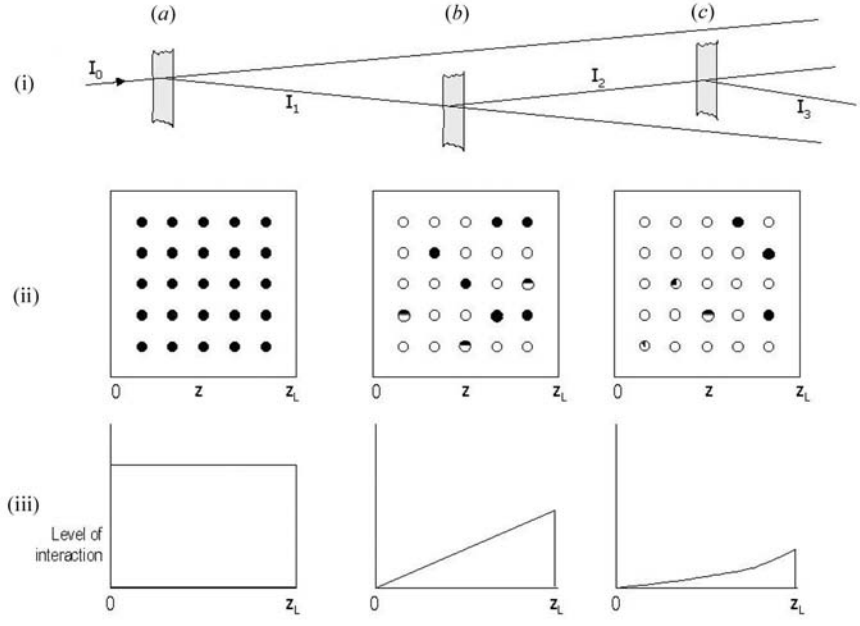

Figure 1
(i) Schematic depiction of the sequence of discrete interactions of a γ-ray beam incident on a series of crystallites in a mosaic crystal. (ii) represents the array of crystallites through the crystal from the entrance face, $z = 0$, to the exit face, $z = z_L$, the level of interaction due to the sequence (*a*) to (*c*) being represented by filled or partially filled circles. (iii) represents the level of interaction from $z = 0$ to $z = z_L$ for the sequence of interactions 1 to 3.

accurate. The curves are fitted to the points to demonstrate the essential trends in the data.]

4. Discussion

The basic reason for extrapolation is to achieve the kinematical limit value of the structure factor from a set of experimental measurements carried out against an appropriate function of a physical variable (Mathieson, 1979). As noted above, the result can depend critically on the function of the variable chosen for extrapolation. The present study illustrates this point dramatically. Palmer & Jauch (1995) assumed a Zachariasen-type relationship, $\gamma(\lambda) = (1 - k\lambda^2)$ and plotted their data against λ^2, deriving limit values for the various F_0^2 which they presented in their Table 2 for the various theoretical models discussed. Our limit values (under MS02) using the same original experimental data (Figs. 2*a* and 2*b*) are compared in Table 3 with those of PJ95 for the Becker & Coppens theoretical model (which appear numerically to be closely allied with the Sabine SAB-P model). It is evident that our procedure consistently leads to higher values. Given the plots in Figs. 2(*a*) and 2(*b*), it is difficult to avoid the conclusion that MS02 corresponds to a more straightforward procedure with clearly defined end points.

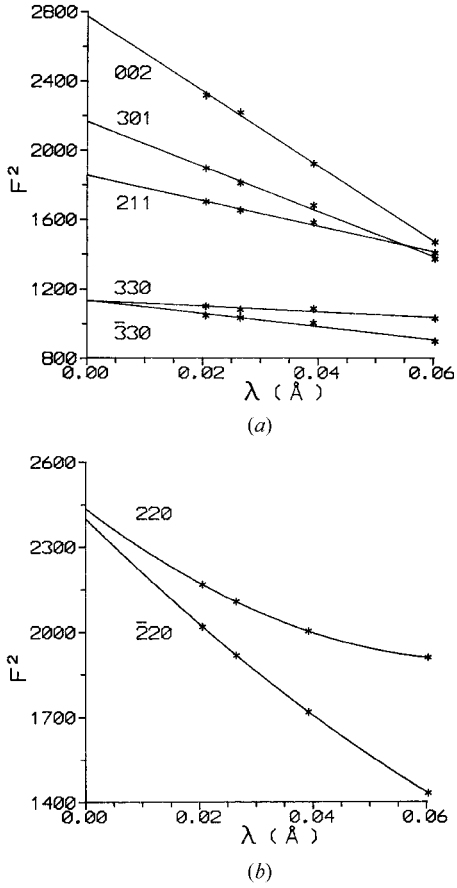

Figure 2
Plots of the experimental F^2 values against λ to yield zero-extinction values. (*a*) for five of the seven reflections, with extrapolation to $\lambda = 0$ of the straight lines, $F^2 = F_0^2 - \alpha\lambda$, fitted to the data points. (*b*) for the two remaining reflections, a symmetry-equivalent pair, with extrapolation to $\lambda = 0$ of the curves, $F^2 = F_0^2 - \alpha\lambda + \beta\lambda^2$, fitted to the data points.

Table 2
For the four wavelengths, F^2_{meas} is compared with F^2_{calc} derived from the formula specified for 220 and $\bar{2}20$, respectively; numerical values of the three contributions to F^2_{calc} are listed.

220	$F^2_{calc} = 2435 - 15293\lambda + 109225\lambda^2$				
λ (Å)	F_0^2	$-\alpha\lambda$	$+\beta\lambda^2$	F^2_{calc}	F^2_{meas}
0.0205	2435	−313.5	+45.9	2167.4	2167
0.0265	2435	−405.3	+76.7	2106.4	2107
0.0392	2435	−599.5	+167.8	2003.3	2003
0.0603	2435	−922.2	+397.2	1910.0	1910

$\bar{2}20$	$F^2_{calc} = 2399 - 19830\lambda + 62532\lambda^2$				
λ (Å)	F_0^2	$-\alpha\lambda$	$+\beta\lambda^2$	F^2_{calc}	F^2_{meas}
0.0205	2399	−406.5	+26.3	2018.8	2019
0.0265	2399	−525.5	+43.9	1917.4	1918
0.0392	2399	−777.3	+96.1	1717.8	1718
0.0603	2399	−1195.7	+227.4	1430.7	1431

Table 3
Comparison of the values of F_0^2 obtained by extrapolation by Palmer & Jauch (1995) and by Mathieson & Stevenson in the present case (MS02), both derived from the original set of F^2 values of PJ95; last column, BK71, is of F_c^2 values calculated with the structural and thermal (harmonic) parameters of NiF_2 determined by Baur & Khan (1971); Σ represents the sum of the F^2 terms.

	PJ95	MS02	BK71
hkl	F_0^2	F_0^2	F_c^2
002	2519	2774	2794
220	2170	2435	2342
$\bar{2}20$	2099	2399	2309
301	1985	2166	2035
211	1739	1854	1784
330	1104	1133	1174
$\bar{3}30$	1077	1134	1150
Σ	12693	13895	13588

Further evidence concerning the absolute level of the kinematical limit values comes from the early structure analysis of NiF_2 by Baur & Khan (1971). With their structural and thermal (harmonic) parameters, F_c^2 values ($\lambda = 0$) for the designated reflections have been calculated with the anomalous dispersion corrections, f' and f'', set to zero. These results are shown in Table 3 under BK71. Since they are calculated values, it is presumed that they represent kinematical limit values (Bragg *et al.*, 1926) and are therefore also zero-extinction values. These values are also consistently larger than those of PJ95. Our impression from examining Palmer & Jauch's experimental results is that the values listed under MS02 more reliably establish the true kinematical limit values for NiF_2.

The reflections 220 and $\bar{2}20$ have several points of interest. For both, the second interaction is, as one would expect, significantly larger than that of the third interaction, as evidenced in Table 2. Of the two, it is $\bar{2}20$ that reveals the greater level of extinction (see Fig. 2*b*), compatible with a larger second component and lesser third component (Table 2). From an experimental point of view, the considerable difference in curvature for the two reflections must be asso-

Table 4
Tabulation of the seven reflections, their extrapolated F_0^2 values, the slope of the α component and the 'experimental' estimate of extinction level for each of the four wavelengths.

			$\gamma = F^2/F_0^2$			
hkl	F_0^2	α (Å^{-1})	λ_1	λ_2	λ_3	λ_4
002	2774	−21637	0.84	0.80	0.69	0.53
301	2166	−13003	0.88	0.84	0.78	0.63
211	1854	−7351	0.92	0.89	0.85	0.76
330	1133	−1629	0.97	0.95	0.96	0.91
$\bar{3}30$	1134	−3979	0.92	0.91	0.88	0.79
220	2435		0.89	0.87	0.82	0.78
$\bar{2}20$	2399		0.84	0.80	0.72	0.60

ciated with their internal morphology. The planes (220) and ($\bar{2}20$) are at right angles so the recorded values must reflect significant differences in the crystallite distortions and mutual misorientations as viewed from the two perspectives. A two-dimensional $\Delta\omega\Delta 2\theta$ investigation of the original crystal specimens carried out at normal wavelengths, *cf.* Mathieson & Stevenson (1986), would probably aid in clarifying the question of the internal morphology.

Concerning 220 and $\bar{2}20$, Palmer & Jauch comment that 'Extrapolations from symmetry-equivalent reflections should lead to identical structure factors in the kinematic limit, $\lambda = 0$, thus providing a strong criterion for an assessment of the fits'. However, in the space group of NiF_2, $P4_2/mmm$, the reflections $hh0$ and $\bar{h}\bar{h}0$ are a symmetry-equivalent Friedel pair but, while $hh0$ and $\bar{h}h0$ are symmetry equivalent, they are not a Friedel pair. The small difference in structure-factor magnitude is associated with a term in the temperature factor. A general discussion of conditions for equivalence of reflections is given by Ibers (1967).

Since the extinction-free values of F_0^2 are derived by extrapolation from experimental data, estimates of the level of extinction, $\gamma = F^2/F_0^2$, are essentially experiment based and may therefore be of interest. These are given in Table 4. α corresponds to the slope of the lines in Fig. 2(*a*), *i.e.* $[F^2(0.06) - F^2(0)]/0.06$.

5. Conclusions

Before one attempts to fit experimental F^2 data to a particular, and possibly inappropriate, relationship, it is worthwhile examining the plot of the experimental F^2 values for each reflection against λ for their trend. There are several possibilities that can be described by the following relationships: (i) $F^2 = (F_0^2 - k_1\lambda)$; (ii) $F^2 = (F_0^2 - k_1\lambda + k_2\lambda^2)$; and (iii) $F^2 = (F_0^2 - k_2\lambda^2)$. The second possibility has a special case, $F = (F_0 - k_1\lambda)$, so that $F^2 = (F_0^2 - 2k_1F_0\lambda + k_1^2\lambda^2)$, $k_i > 0$. These relationships are associated with the following trends. The first, obviously, is a straight line (as in Fig. 2*a*). The second is concave upwards (as in Fig. 2*b*). The third is concave downwards and corresponds to a Zachariasen-derived relationship (see PJ95, p. 665).

One can therefore judge, purely from the experimental trend for the individual reflection, which general case applies. On this basis, one can carry out the extrapolation for each reflection almost wholly from the experimental results as we have performed in Figs. 2(*a*) and 2(*b*). The better the quality of the data, the more clearly defined is the trend and the more precisely established is the extrapolation limit. In this respect, the multiwavelength data of Palmer & Jauch (1995) are outstanding.

It is interesting to note that Hester & Okamura (1996) carried out multiwavelength measurements on a crystal of K_2PdCl_4 over the range 0.11–0.25 Å. They plotted their results as *F versus* λ, which they pointed out corresponds to a straight line. As we note above, this result is equivalent to $F^2 = (F_0^2 - \alpha\lambda + \beta\lambda^2)$ and their observations appear to extend the wavelength range of this formula beyond the γ-ray region into the lower limits of the more classical X-ray range.

Multiwavelength γ-ray measurement appears capable of providing information on the sequence of diffraction interactions, which suggests that this discontinuous model warrants further investigation.

We are most grateful to Drs A. Pogany and S. W. Wilkins for valuable suggestions arising from their reading of the text.

References

Baur, W. H. & Khan, A. A. (1971). *Acta Cryst.* B**27**, 2133–2139.
Becker, P. J. & Coppens, P. (1975). *Acta Cryst.* A**31**, 417–425.
Bragg, W. L., Darwin, C. G. & James, R. W. (1926). *Philos. Mag.* **1**, 897–922.
Buerger, J. M. (1942). *X-ray Crystallography*, ch. 20. New York: Wiley.
Darwin, C. G. (1922). *Philos. Mag.* **43**, 800–829.
Hester, J. R. & Okamura, F. P. (1996). *Acta Cryst.* A**52**, 700–704.
Ibers, J. A. (1967). *Acta Cryst.* **22**, 604– 605.
James, R. W. (1948). *The Optical Principles of the Diffraction of X-rays*, p. 536. London: Bell.
Kettmann, G. (1929). *Z. Phys.* **53**, 198–209.
Mackenzie, J. K. & Mathieson, A. McL. (1979). *Acta Cryst.* A**35**, 45–50.
Mackenzie, J. K. & Mathieson, A. McL. (1984). *Aust. J. Phys.* **37**, 651–656.
Mathieson, A. McL. (1979). *Acta Cryst.* A**35**, 50–57.
Mathieson, A. McL. & Stevenson, A. W. (1986). *Acta Cryst.* A**42**, 223–230.
Palmer, A. & Jauch, W. (1995). *Acta Cryst.* A**51**, 662–667.
Sabine, T. M. (1992). *International Tables for Crystallography*, Vol. C, pp. 530–533. Dordrecht: Kluwer.
Wilson, A. J. C. (1949). *X-ray Optics – the Diffraction of X-rays by Finite and Imperfect Crystals*, p. 4. London: Methuen.
Zachariasen, W. H. (1967). *Acta Cryst.* **23**, 558–564.